INL/RPT-23-74791

Results of FY 2023 Alloy 617 and Alloy 709 High-Temperature Crack-Growth Testing

September 2023

Michael D. McMurtrey, Michael P. Heighes, and Cody J. Gibson
Idaho National Laboratory

Idaho National Laboratory

INL/RPT-23-74791

Results of FY 2023 Alloy 617 and Alloy 709 High-Temperature Crack-Growth Testing

Michael D. McMurtrey, Michael P. Heighes, and Cody J. Gibson
Idaho National Laboratory

September 2023

Idaho National Laboratory
Advanced Reactor Technologies
Idaho Falls, Idaho 83415

http://www.art.inl.gov

Prepared for the
U.S. Department of Energy
Office of Nuclear Energy
Under DOE Idaho Operations Office
Contract DE-AC07-05ID14517

Page intentionally left blank

INL ART Program

Results of FY23 Alloy 617 and Alloy 709 High Temperature Crack Growth Testing

INL/RPT-23-74791

September 2023

Technical Reviewer: (Confirmation of mathematical accuracy, and correctness of data and appropriateness of assumptions.)

Heramb Mahajan Materials Scientist	09-19-2023 Date

Approved by:

Michael E. Davenport ART Project Manager	9/20/2023 Date
Travis R. Mitchell ART Program Manager	9/20/2023 Date
Michelle T. Sharp INL Quality Assurance	9/20/2023 Date

Page intentionally left blank

ABSTRACT

This report summarizes the work performed this year at Idaho National Laboratory to validate the crack-growth monitoring setup used with the test frames against both continuous crack length monitoring using an optical camera, as well as post-mortem analysis of marker bands on the fracture surface. Delays prevented the use of a gauge to measure load line displacement for early tests, and so the creep-fatigue crack-growth setup was evaluated using the actuator displacement for a load line displacement setup. While not ideal, this allowed examination of the shortcomings with the current software setup that was originally designed for performing stress corrosion crack-growth rate studies. The method for data collection was modified to link the crack-growth monitoring software with Instron's Wave Matrix software. Once the load line displacement gauge arrived, the crack-growth equipment was successfully modified to permit continuous monitoring of both load line displacement and crack length. This is critical for creep-fatigue and creep crack-growth rate studies for ductile material, as it permits the C* and C_t analyses. Test results are shown for Alloy 617 fatigue and creep-fatigue (without the gauge for load line displacement measurements), as well as creep-fatigue of Alloy 709, which was performed with the completed test setup, allowing for crack length and load line displacement monitoring.

Page intentionally left blank

ACKNOWLEDGEMENTS

This work was sponsored by the United States (U.S.) Department of Energy (DOE) under Contract No. DE-AC07-05ID14517 with Idaho National Laboratory (INL), which is managed by Battelle Energy Alliance. Programmatic direction was provided by the Office of Nuclear Reactor Deployment of the DOE Office of Nuclear Energy. The authors gratefully acknowledge the support provided by Sue Lesica, the Federal Lead for Advanced Materials of the Advanced Reactor Technologies (ART) Program. The authors thank Gerhard Strydom, the National Technical Director of the ART Gas-Cooled Reactors Campaign. Additionally, the authors thank Ting-Leung Sham, the ART Materials Technical Area Lead, for his substantial support of this project. Lastly, the authors also acknowledge the technical support from Joel Simpson of INL.

Page intentionally left blank

CONTENTS

FIGURES

TABLES

Page intentionally left blank

ACRONYMS

ART	Advanced Reactor Technologies
ASME	American Society of Mechanical Engineers
ASTM	American Society for Testing and Materials
ATI	Allegheny Technologies Incorporated
BPVC	Boiler and Pressure Vessel Code
CGR	crack-growth rate
COD	crack opening displacement
CT	compact tension
DCPD	direct current potential drop
DOE	Department of Energy
INL	Idaho National Laboratory

Page intentionally left blank

Results of FY 2023 Alloy 617 and Alloy 709 High-Temperature Crack-Growth Testing

1. INTRODUCTION

Alloy 617 was recently added to the American Society of Mechanical Engineers (ASME) Boiler and Pressure Vessel Code (BPVC) [1] through a Code Case in Section III, Division 5, permitting it for use in Class A high-temperature nuclear components [2]. Alloy 709 is currently being tested to gather data for a Section III, Division 5 Code Case as well [3]. These Code Cases represent a significant amount of testing, such as tensile, creep, fatigue, and creep-fatigue, that generate the data used for the development of design parameters for design evaluations. While Section III, Division 5 provides rules for construction for high-temperature nuclear components, it does not provide guidance for in-service inspection or monitoring of components during their lifetimes in operation. This falls under ASME BPVC Section XI [1], which covers rules for in-service inspections of nuclear power plant components. Division 2 of Section XI specifically covers requirements for reliability and integrity management programs for advanced reactors.

During operation of components, it is critical to understand how flaws and defects grow during normal operation under loads (include cyclic), coolant environments particular to the reactor design, and at high temperature. Section XI of the ASME BPVC requires information on crack-growth behaviors, which are not examined under Section III, Division 5. Relevant crack-growth rate (CGR) testing to high-temperature nuclear materials falls under three American Society for Testing Materials (ASTM) Standards: ASTM E647 [4], ASTM E1457 [5], and ASTM E2760 [6], covering fatigue, creep, and creep-fatigue CGR testing, respectively. A brief description of these testing standards is provided below.

Fatigue CGRs (da/dN, with a referring to the crack length and N the number of fatigue cycles) are compiled as a function of crack-tip stress-intensity factor range (ΔK). The specimen must be thick enough to ensure that buckling does not occur and the small-scale yielding conditions are maintained for using the linear elastic fracture mechanics approach. CGRs must be measured during the test, as crack size is directly linked to K, which serves as the control variable.

Creep CGR testing is performed under static or quasi-static loading conditions at elevated temperatures where creep deformation occurs. In this case, creep crack growth is measured in da/dt (change in crack length over change in time) usually as a function of K, Ct or C* where Ct and C* are the transient and steady-state crack-tip characterizing parameters under the creep condition. The C* parameter is valid only when extensive creeping condition is obtained. The exact choice of parameter to correlate with crack growth depends on the creep properties (creep-ductile or creep-brittle) as well as the specimen geometry. For creep CGR testing, loads and temperatures are set, and crack length history, as well as load line displacement measurements are continuously recorded during the test.

Creep-fatigue CGRs seek to capture the time-dependent intergranular creep and cycle-dependent transgranular fatigue, and their interactions. The complicated interaction between these two cracking mechanisms is affected by the material, cyclic loading frequency, and the shape of the load cycle. These parameters simulate the components under in-service conditions. As with creep CGRs, the creep portion of the creep-fatigue testing can exhibit creep-ductile or creep-brittle behavior. Creep-fatigue CGRs are expressed in terms of da/dN expressed in terms of ΔK for creep-brittle materials and da/dt expressed in terms of C_t or C* for creep-ductile materials. The C_t parameter is used to characterize creep CGRs under a wide range of conditions from small-scale to extensive steady-state creep; therefore, it is a time-dependent parameter, and it approaches C* under extensive creep condition. As with C*, continuous monitoring of load line displacement is needed to evaluate C_t, as well as a means for continuous monitoring of the crack length.

All three CGR testing types typically use a compact tension (CT) type specimen. The importance of each data set is determined by the expected conditions of the component. Where heavy cyclic loading is expected for the component or structure, fatigue CGRs are useful in assessment of cracks (and crack-like defects). Where load/stress is expected to be relatively constant and the component will operate at an elevated temperature, creep CGRs are used in the assessment. Where components experience elevated temperature as well as slow moving cyclic loads, or load where cycles are interrupted with hold times, creep-fatigue CGRs are relevant.

This report covers the work performed at Idaho National Laboratory (INL) during fiscal year (FY) 2023 on high-temperature crack-growth testing for Alloy 617 and Alloy 709 to support ASME Section XI Division 2 code cases. Prior work at INL, primarily on Alloy 617, has been reported previously in Bass's 2022 report and Benz and Wright's 2013 conference paper [7,8]. In the previous studies, the effects of material processing (aged, carburized, solution annealed), temperature (650°C and 800°C), environment (air and impure helium), and fatigue loading (frequency and magnitude) were examined using constant K tests.

In the previous work, load line displacement was not measured. This is not a concern for fatigue CGRs, where ΔK was used to evaluate the CGRs; however, for processes involving creep (creep and creep-fatigue CGRs), this implies that the material was creep-brittle and so ΔK was relevant. There are concerns that this assumption does not match the actual behavior of Alloy 617, and so this work will continue the work of evaluating Alloy 617 (and initiating work at INL on Alloy 709) using C* and C_t. This work builds on the prior work, setting up the INL mechanical test systems to permit both crack-growth and load line displacement measurements to gather data in support of the Section XI high-temperature flaw evaluation method.

2. EXPERIMENTAL SETUP

2.1. Materials

The Alloy 617 plate used in this work was produced by ThyssenKrupp Vereinigte Deutsche Metallwerke, Heat 314626. The chemical composition of this heat is provided in Table 1. The significant strengthening mechanisms in Alloy 617 are solid solution strengthening from Co and Mo as well as precipitation strengthening. The main precipitates, which can result in strengthening in Alloy 617, are $M_{23}C_6$, M_6C, and various Ti-containing precipitates. The Alloy 709 plate was produced by Allegheny Technologies Incorporated (ATI), Heat CG45192. Alloy 709 is a high-strength stainless steel that is precipitation strengthened by the addition of niobium.

Table 1. Alloy 617 Heat 314626 and Alloy 709 Heat CG45192 compositions (in weight percent).

	Ni	Cr	Co	Mo	Fe	Mn	Al	C	N	Cu	Si	S	Ti	Nb	B	P
617	54.1	22.2	11.6	8.6	1.6	0.1	1.1	0.05	–	0.04	0.1	<0.002	0.4	–	<0.001	–
709	25.0	19.8	0.01	1.5	Bal.	0.9	0.02	0.07	0.15	0.04	0.44	0.001	<0.01	0.18	0.005	0.008

2.2. Specimens

Early work on this project used the same specimen design as used in the previous INL CGR testing. This is a standard 1/2-in.-thick CT specimen, shown in Figure 1a. This specimen design is often used for fatigue and stress corrosion CGR studies. It does not permit the use of an extensometer to measure the load line displacement, and so for the creep and creep-fatigue studies to be performed in this work, the specimen was redesigned with notches to permit an extensometer to connect to the specimen on the load line, shown in Figure 1b and Figure 1c. Both specimen designs permit the use of direct current potential drop (DCPD) wires to be welded on to the front face, spanning across the machined mouth/notch from where the crack will initiate and propagate. DCPD is a method of continuously monitoring the crack length and will be described in the following section on test setup.

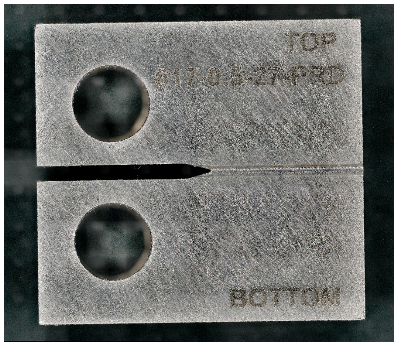

(a)

(b)

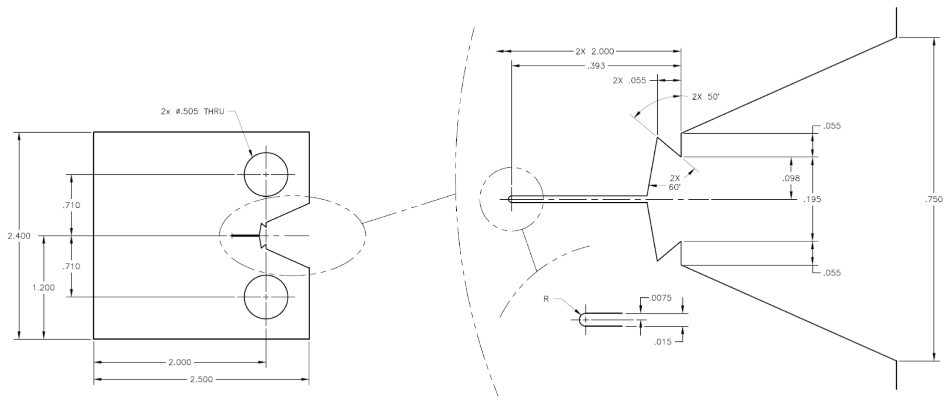

(c)

Figure 1. (a) Standard CT specimens used in previous INL work as well as early work within this project. (b) Redesigned CT specimens to permit load line displacement measurements, with details shown more clearly in (c).

2.3. Crack-Growth Rate Test Setup

Crack-growth testing utilizes a test frame, furnace, and DCPD system to apply constant stress intensities to the CT specimens, as well as an extensometer when load line displacement is monitored. The furnace attached to the test frame has a maximum temperature of 1000°C. INL has performed crack-growth testing in the past, but the equipment needed upgrades, which began last year. A new Epsilon Model 3548 crack opening displacement (COD) gauge with 5-mm gauge length and +10-mm range was procured and installed on the Strain 1 channel for each of the Instron 8862 load frame to measure load line displacement more accurately. The Instron 8862 electromechanical load frames with 100-kN Dynacell load cells were calibrated and returned to service. DCPD systems, previously used for stress corrosion cracking, that consist of a calibrated Agilent 6611C power supply, calibrated Agilent 34420 Nanovoltmeter, Agilent 34970 Data Acquisition Unit, and INL-manufactured current switching box were set up on each frame an updated to work with current windows software. Figure 2 shows the testing setup with both DCPD wires welded on to the specimen, as well as the COD gauge for load line displacement measurements.

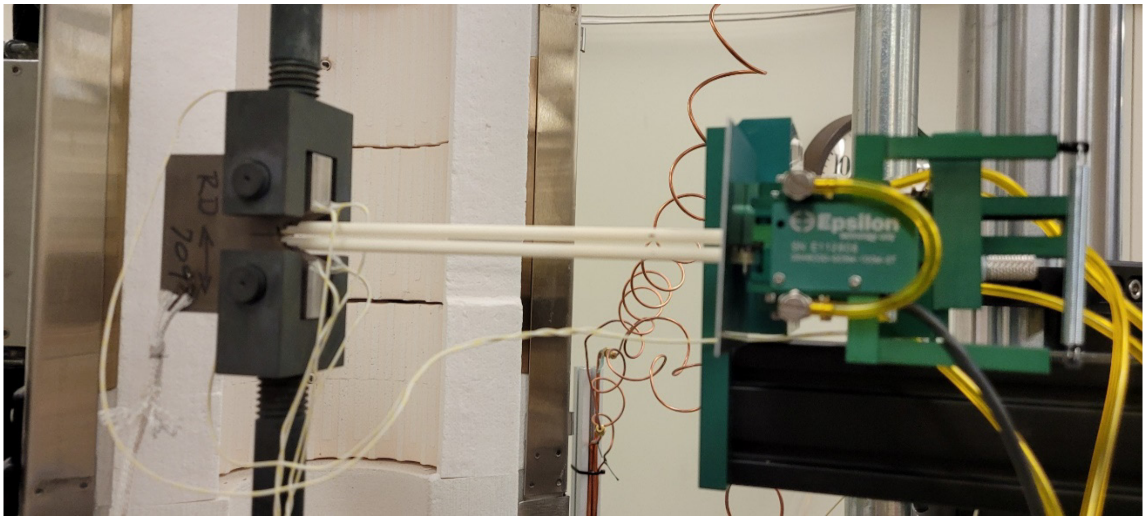

Figure 2. CGR testing setup with DCPD and load line displacement extensometer.

2.4. Delays in Work in FY 2023

Several delays occurred in FY 2023 that slowed progress on this work or required addition time/effort to overcome. Procurement of the load line displacement extensometer was significantly delayed, with the extensometer not arriving at INL until May 2023, reducing the amount of time that testing with the extensometer could be performed. There was also an issue with the Instron load frame that was initially set up for testing these specimens in air environment at elevated temperatures. The Instron 8800 control tower that manages the data acquisition from the 8862 electrotechnical frame lost power and would not return to service, requiring a field service visit by Instron to diagnose the system. This led to all creep-fatigue CGR testing being diverted to a different load frame which required changes to the frame as it was previously set up for high-temperature gas environment testing and would not accommodate the Epsilon COD extensometer and ASTM 2760 standard size specimens.

3. RESULTS

3.1. Fatigue Crack-Growth Rate Testing

Due to delays in the arrival of the load line displacement extensometer, further examination of the DCPD results was performed to ensure accuracy of the measurements. A marker banding test was performed on an Alloy 617 CT specimen in fatigue, where marker bands are placed in the fracture surface by changing K_{max} and R (the ratio of maximum and minimum loads in the fatigue cycle). These changes to the loading cycle create visible marks on the fracture surface at set times within the experiment that allows a more accurate examination of crack length by post-mortem examination of the fracture surface. The test was run at room temperature, with a K_{max} of 25 MPa√m, an R of 0.1, and a frequency of 1 Hz during the pre-crack and normal CGR portions of the test. The marker bands were run at a K_{max} of 29 MPa√m, an R of 0.7, and a frequency of 1 Hz. A secondary method for continuous crack length monitoring was also employed, using an optical camera to image the specimen during the loading cycles and to visually monitor the crack development, as shown in Figure 3. These two methods were compared to the DCPD results with the marker bands, shown in Figure 3c, acting as the true crack length measurement.

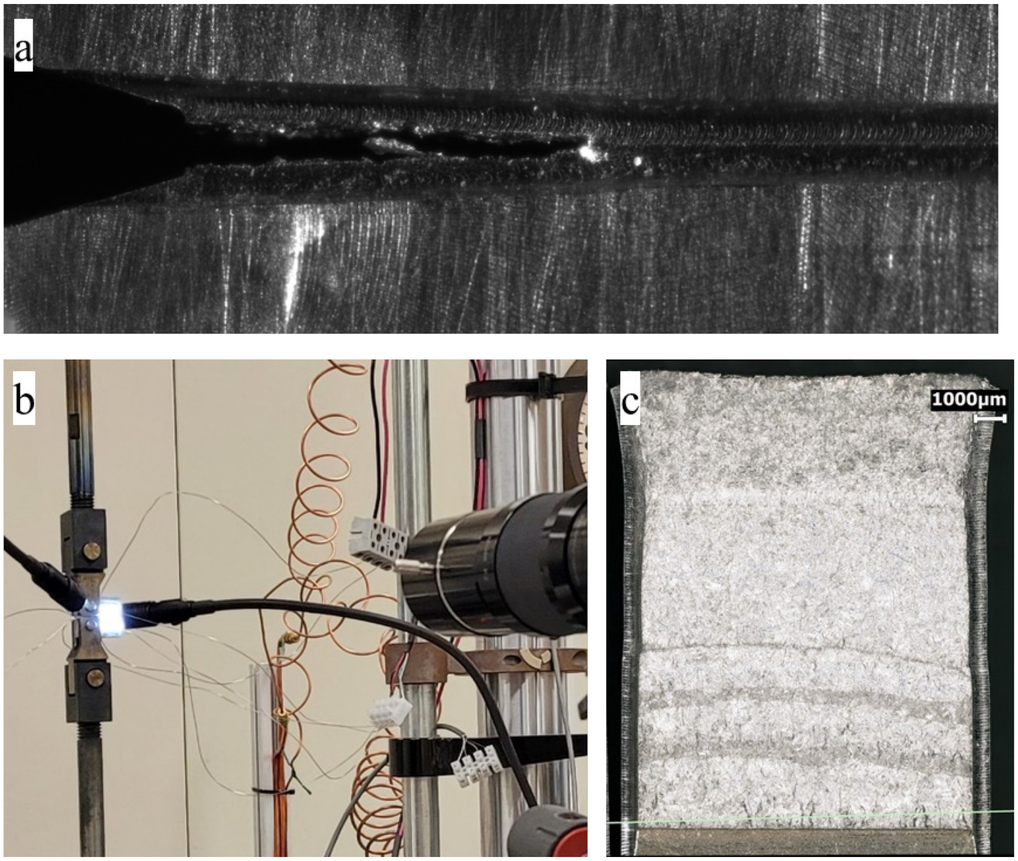

Figure 3. Testing performed to examine the accuracy of the DCPD measurement setup. Crack length was viewed from the side of the specimen during testing (a) using a camera and light setup shown in (b). Marker bands from varying Kmax and R values allowed for direct measurements of crack length on the fracture surface (c) after the completion of the test.

The various measurements for crack length, as well as calculated values, are shown in Figure 4. Six different values are shown in the graph, as described below.

- *a* – calculated directly from DCPD.
- Corrected *a* – calibrated *a*, using initial and final crack length measurements to create a correction factor in accordance with ASTM E2760 Section A2.1, shown in Equation (1) [6].

$$a = \left[(a_f - a_0)\frac{(U-U_0)}{(U_f-U_0)}\right] + a_0 \quad (1)$$

where:

a = crack length

a_f and a_0 = final and initial crack lengths

U = DCPD potential drop

U_f and U_o = the potential drop at the final and initial crack lengths.

- Fracture surface – Average measurements from the fracture surface micrographs.
- Optical camera – Measured from the optical camera.

- Calculated based on ASTM 2760 correlations, following Equation (2) (Equation A2.2 in ASTM E2760) [6].

$$\frac{a}{W} = \frac{2}{\pi} cos^{-1}\left[\frac{\cosh(\ \pi Y_0/2W)}{cosh\left[\frac{U}{U_0}\right]cosh^{-1}\left\{\frac{cosh(\pi Y_0/2W)}{cos(\pi a_0/2W)}\right\}}\right] \tag{2}$$

where:

a and a_0	=	the crack length and initial crack length
W	=	width of the CT specimen from the load line to the end of the specimen
U	=	output voltage
U_0	=	DCPD potential drop at the initial crack length
Y_0	=	half the distance between the output voltage leads.

- Calculated based on ASTM 647 correlations, following Equation (3) (Equation A1.6 in ASTM E647) [4].

$$a/W = B_0 + B_1(V/V_r) + B_2(V/V_r)^2 + B_3(V/V_r)^3 \tag{3}$$

where:

a	=	crack length
W	=	width of the specimen from load line to the end
V	=	potential drop
V_r	=	reference crack voltage for when a/W = 0.241.

Constant values for B_0-B_3 are provided in ASTM E647 [4].

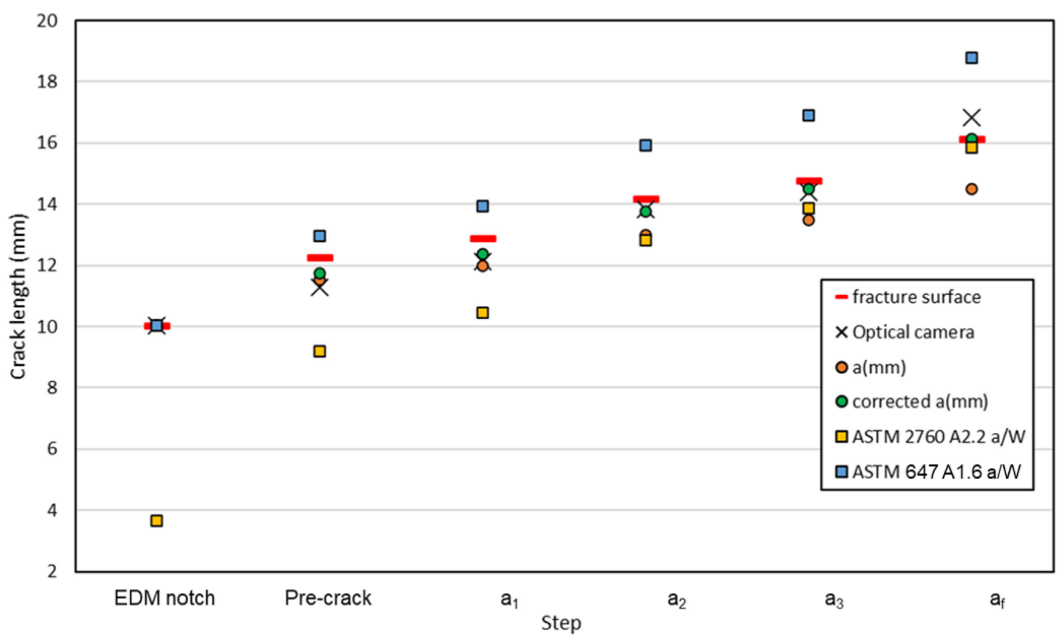

Figure 4. Six crack length measurements calculated and measured through different methods for comparison.

Overall, measurements generally agree with the fracture surface measurements, with the ASTM 2760 being the greatest outlier, particular for earlier cracking stages. While the fracture surface measurements permitted for direct, post-mortem, measurements of the crack length at known numbers of cycles, the crack front, as seen in Figure 3c, is not flat. To account for this, an average crack length was used with multiple measurements taken across the thickness of the specimen. The optical camera only permits the side of the crack to be seen, and so with the curvature of the crack front, it is expected that the optical camera should give an accurate or shorter crack length measurement, which is the case for all points except the final crack length. It is not clear why the optical camera measurement was longer for the final crack length measurement; however, this was likely human error in interpreting the images, as the crack tip was not always clearly visible in the optical images. As expected, the corrected *a* values from the DCPD measurements are more accurate than the *a* values directly calculated, as the corrected *a* includes a linear correction based on the initial and final crack length measurements (final crack length measurement taken post-mortem). It is important to see the difference between *a* and correct *a*, as the *a* values are used during the test to calculate K for the K controlled test. A corrected K value is calculated post-mortem; however, if the *a* value has deviated too far from the true crack length, then there will be excessive error between the K the test was controlled to and the true K values. There are significant errors for the ASTM E647 and ASTM E2760 values as the specimen geometry used (Figure 1a) was used for INL stress corrosion cracking testing and does not meet the standard geometry requirements for either of these standards. The redesigned specimens shown in Figure 1b and Figure 1c do meet the standard geometry requirements.

3.2. Preliminary Creep-Fatigue Crack-Growth Rate Testing

To ensure a smooth transition to creep-fatigue testing a preliminary creep-fatigue test was performed to test the software when the extensometer arrived. This preliminary test was performed using load line displacement as measured by the actuator displacement. Load line displacement by actuator movement is not ideal, given the amount of compliance typically in the load train; however, it permitted the test to be run prior to the arrival of the extensometer. The DCPD system used was initially set up for use on stress corrosion cracking testing systems, and not intended for the high-data collection rate of load and position associated with creep-fatigue CGR cyclic testing. Concerns were associated with the DCPD system's ability to acquire the cyclic loading and position data at a high enough rate to discern each individual loading cycle. The data recording was an average of several DCPD readings performed during longer time increments (as is appropriate for stress corrosion cracking, where crack growth is quite slow). The specimen was pre-cracked at room temperature at a K_{max} of 25 MPa√m, an R of 0.1, and a frequency of 1 Hz. Following the pre-crack, the creep-fatigue CGR test was performed at 800°C, with a K_{max} of 25 MPa√m, an R of 0.1, a frequency of 1 Hz, with a 10-sec hold time at peak load. Beach markers were placed in the sample using the exact same parameters, but without the hold time (hold time was set to 0 sec). The results are shown in Figure 5–Figure 7.

Figure 5. Fracture surface of Alloy 617 specimen used for the preliminary creep-fatigue test.

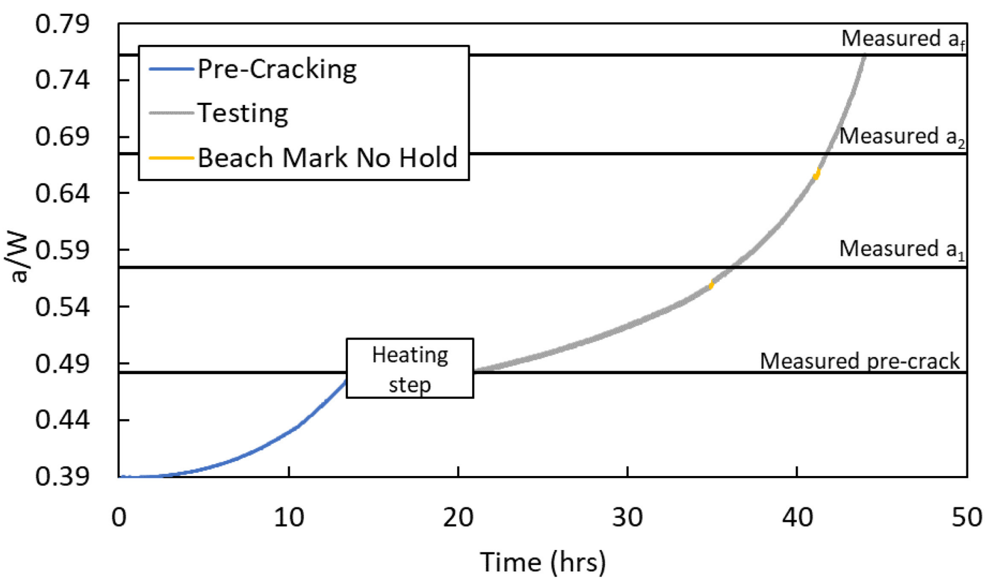

Figure 6. Crack length results from the preliminary creep-fatigue test. Crack length is normalized to W, the width of the CT specimen (from the load line to the far end of the specimen). The adjusted *a* is used

for the *a*/W calculation, which is corrected to the post-mortem measured pre-crack length and final crack length.

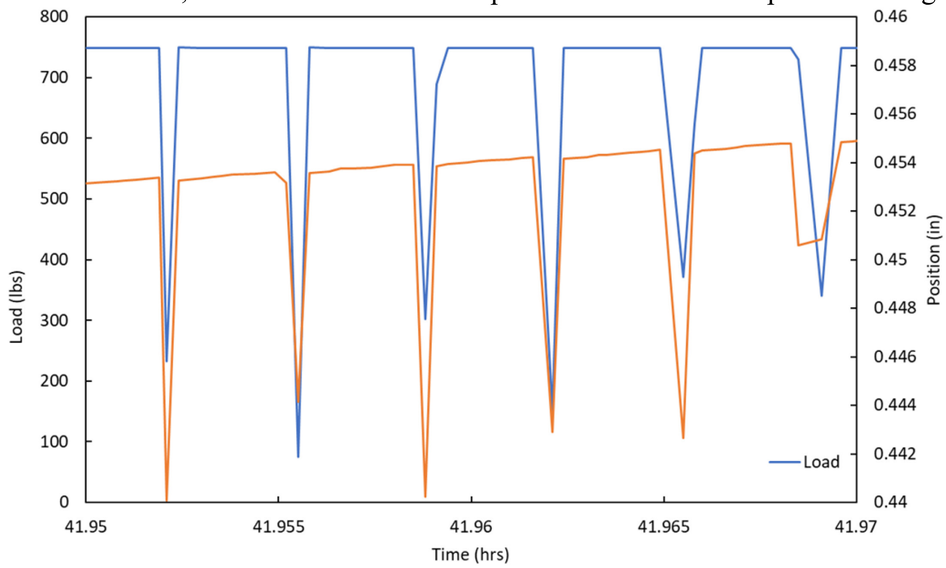

Figure 7. Load and load line displacement (as measured by the actuator) for the preliminary creep-fatigue test.

Overall, this test was not considered successful, for the expected reasons. The load line displacement as measured by the actuator displacement was not accurate enough to be useful. More importantly, the DCPD software could not collect the data fast enough to capture minimum loads in the fatigue cycles. This is seen in Figure 7, where the minimum load appears to change each cycle, though the test was controlled to a set minimum load. Maximum load was successfully captured, due to the hold time at that load. In this sense, the test was successful in highlighting the modifications needed for the creep-fatigue test to ensure the required data was collected. As seen previously, there is some error between the adjusted *a* values and the post-mortem marker-band measurements.

The concern with DCPD data is due to the INL setup being primarily used for stress corrosion cracking testing where the load is maintained at a certain stress concentration at the crack tip; therefore, only adjusted load based on defined averages of DCPD data to perform load corrections throughout the test to maintain a constant K. It was determined that the DCPD system could be used to collect crack-growth data at a higher rate if load control was maintained with Instron software. Therefore, on the ASTM E2760-sized specimen DCPD load control was used to maintain a constant K value for pre-crack fatigue and then stopped when the specimen reached the desired pre-crack length. Then after the specimen was raised to the desired testing temperature, Instron Wave Matrix software was used to control load cycling and to collect load and displacement data at a rate of 5 Hz that would accurately capture the minimum loads during fatigue cycles. The DCPD system only collected voltage potentials off the specimen to calculate crack length and correlate to each fatigue cycle based on computer time stamp.

3.3. Complete Creep-Fatigue Crack-Growth Rate Testing

With the arrival of the extensometer, it was possible to perform complete creep-fatigue CGR testing with DCPD continuously monitoring crack length, and the extensometer continuously monitoring load line displacement. Two tests were performed, a trial test using an Alloy 718 specimen to perform a shakedown on the equipment, and a preliminary test performed on Alloy 709 to demonstrate the creep-fatigue setup on the alloy of interest for this work. The Alloy 718 demonstrated that the new COD gauge data could be collected simultaneously with the DCPD, following the setup described in Section 3.2 of this report.

The Alloy 709 creep-fatigue test is currently running (current results shown in Figure 8). It has been programmed with the following steps:

- A room temperature pre-crack performed at constant K = 25 R = 0.1 F = 1Hz Hold = 0s to an a/W = 0.28140.
- Followed by a room temperature pre-crack performed at constant K=30 R=0.1 F=1Hz Hold=0s to an a/W=0.34070.
- The temperature was then increased to 600°C.
- (Creep-fatigue step) Cycling started with 1-sec ramp to the maximum load of 2831 lbf, and a hold time of 60 sec, followed by a 1-sec ramp down to the minimum load of 283.1 lbf (R=0.1) for 2500 cycles.
- (Fatigue step) After 2500 cycles of the previous step is reached, the program switches to cycling with a 1-sec ramp to the maximum load of 2831 lbf, with a hold time of 0 sec, followed by a 1-sec ramp down to a minimum load of 283.1 lbf for 5000 cycles.
- Repeat the last two steps 10 times or until creep crack growth takes over fatigue crack propagation.

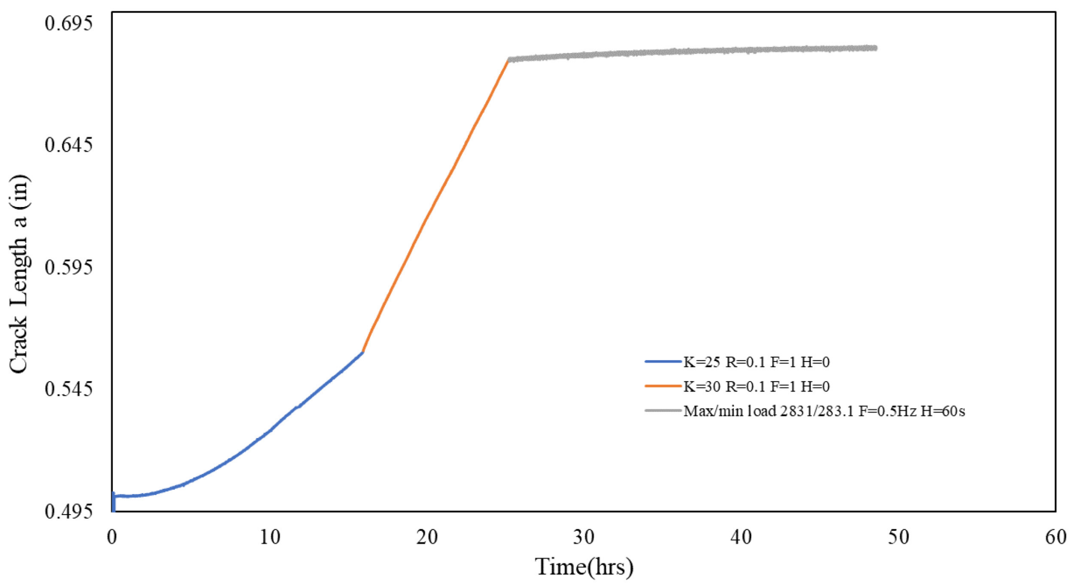

Figure 8. Crack length versus time of Alloy 709 creep-fatigue test. The test is currently ongoing.

Once more, data has been collected on the Alloy 709 test, a C_t analysis will be performed to analyze the cracking behavior with respect to C_t. This will represent the first full creep-fatigue crack-growth analysis performed at INL using both DCPD to monitor crack-growth behavior as well the COD gauge to monitor load line displacement.

4. SUMMARY

The work performed this year validated the DCPD crack-growth monitoring setup used with the INL test frames against both continuous crack length monitoring using an optical camera, as well as post-mortem analysis of marker bands on the fracture surface. Delays prevented the use of a COD gauge for early tests, so the creep-fatigue crack-growth setup was evaluated using the actuator displacement for a load line displacement setup. While not ideal, this allowed examination of the shortcomings with the current software setup that was originally designed for performing stress corrosion CGR studies. The method for data collection was modified to link the DCPD crack-growth monitoring software with Instron's Wave Matrix software. Once the COD gauge arrived, INL's crack-growth equipment was successfully modified to permit continuous monitoring of both load line displacement and crack length. This is critical for creep-fatigue and creep CGR studies for ductile material, as it permits the C* and C_t analyses. Future work will continue to investigate the creep-fatigue and initiate work on creep CGRs of Alloys 617 and 709 in air, as well as to initiate testing in impure helium, to examine CGRs in prototypical gas-cooled reactor environments.

5. REFERENCES

1. ASME. 2023. "Boiler and Pressure Vessel Code (BPVC)." American Society of Mechanical Engineers, New York, NY.
2. ASME. 2023. "Boiler and Pressure Vessel Code (BPVC)." Code Case N-898, American Society of Mechanical Engineers, New York, NY.
3. Sham, T.-L., Y. Wang, R. Bass, X. Zhang. 2022. "A709 Qualification Plan Update and Mechanical Properties Data Assessment." INL/RPT-22-67641, Idaho National Laboratory, Idaho Falls, ID. https://www.osti.gov/servlets/purl/1906516.
4. ASTM. 2023. "Standard Test Method for Measurement of Fatigue Crack Growth Rates." ASTM E647-23a, ASTM International, West Conshohocken, PA.
5. ASTM. 2022. "Standard Test Method for Measurement of Creep Crack Growth Times in Metals." ASTM E1457-19e1, ASTM International, West Conshohocken. PA.
6. ASTM. 2020. "Standard Test Method for Creep-Fatigue Crack Growth Testing." ASTM E2760-19e1, ASTM International, West Conshohocken, PA.
7. Bass, J. 2022. "Results of Initial Alloy 617 High Temperature Crack Growth Testing." INL/RPT-22-69322, Rev. 0, Idaho National Laboratory. September 2022. https://inldigitallibrary.inl.gov/sites/sti/sti/Sort_63641.pdf.
8. Benz, J. and R. Wright. 2013. "Fatigue and Creep Crack Propagation behaviour of Alloy 617in the Annealed and Aged Conditions." INL/CON-13-30214, in proceedings of the Third International Workshop on Structural Materials for Innovative Nuclear Systems, Idaho Falls, ID. https://www.osti.gov/servlets/purl/1111504.